Early prognosticators of later TSPO-PET-measurable microglial activation in multiple sclerosis

Laaksonen, S.; Saraste, M.; Sucksdorff, M.; Nylund, M.; Vuorimaa, A.; Matilainen, M.; Heikkinen, J.; Airas, L.

Published in:
Multiple Sclerosis and Related Disorders

DOI:
10.1016/j.msard.2023.104755

Published: 01/07/2023

Document Version
Final published version

Document License
CC BY

Multiple Sclerosis and Related Disorders 75 (2023) 104755

Contents lists available at ScienceDirect

Multiple Sclerosis and Related Disorders

journal homepage: www.elsevier.com/locate/msard

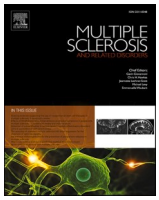

Original article

Early prognosticators of later TSPO-PET-measurable microglial activation in multiple sclerosis

S Laaksonen [a,b,c,*], M Saraste [a,b,c], M Sucksdorff [a,b,c], M Nylund [a,b,c], A Vuorimaa [a,b,c], M Matilainen [a,d], J Heikkinen [e], L Airas [a,b,c]

[a] Turku PET Centre, Turku University Hospital and University of Turku, Turku, Finland
[b] Division of Clinical Neurosciences, University of Turku, Turku, Finland
[c] Neurocenter Turku, University Hospital, Turku, Finland
[d] Faculty of Science and Engineering, Åbo Akademi University, Turku, Finland
[e] Department of Radiology, University of Turku and Turku University Hospital, Turku, Finland

ARTICLE INFO

Keywords:
Positron-emission tomography
TSPO
Microglia
Progressive multiple sclerosis
T2-lesion
Immunoglobulin G index

ABSTRACT

Background: Factors driving increased innate immune cell activation in multiple sclerosis (MS) brain are not well understood. As higher prevalence of microglial/macrophage activation in association with chronic lesions and diffusely in the normal appearing white matter predict more rapid accumulation of clinical disability, it is of high importance to understand processes behind this. Objective of the study was to explore demographic, clinical and paraclinical variables associating with later positron emission tomography (PET)-measurable innate immune cell activation.

Methods: PET-imaging using a TSPO-binding [^{11}C]PK11195 was performed to evaluate microglial activation in patients with relapsing-remitting MS aged 40-55 years with a minimum disease duration of five years (n = 37). Medical records and diagnostic MR images were reviewed for relevant early MS disease-related clinical and paraclinical parameters.

Results: More prominent microglial activation was associated with higher number of T2 lesions in the diagnostic MRI, a higher immunoglobulin G (IgG) index in the diagnostic CSF and Expanded Disability Status Scale (EDSS) $\geq$ 2.0 five years after diagnosis.

Conclusion: The number of T2 lesions in MRI, and CSF immunoglobulin content measured by IgG index at the time of MS diagnosis associated with later TSPO-PET-measurable innate immune cell activation. This suggests that both focal and diffuse early inflammatory phenomena impact the development of later progression-related pathology.

1. Introduction

Innate immune cell activation in the central nervous system (CNS) is a prominent pathological feature of multiple sclerosis (MS) which can be assessed *in vivo* using positron emission tomography (PET)-imaging and radioligands binding to the 18 kDa translocator protein (TSPO) (Banati et al., 2000; Giannetti et al., 2015; Rissanen et al., 2014). Compared to healthy controls (HC), MS-patients display increased TSPO-PET-measurable microglial activation in the normal appearing white matter (NAWM) and in thalamus (Rissanen et al., 2018). This phenomenon is most pronounced in advanced MS, and increased TSPO-binding also predicts later disease progression (Sucksdorff et al., 2020). Microglia and macrophage activation at the edge of chronic lesions and in the NAWM associate with MS disease type, disease severity and future progression, but factors promoting and maintaining the increased innate immune cell activation in MS brain are largely unknown (Frischer et al., 2015; Lassmann, 2018; Luchetti et al., 2018).

In early MS, peripherally activated T cells enter the CNS through

Abbreviations: MS, multiple sclerosis; PET, positron emission tomography; TSPO, translocator protein; HC, healthy control; NAWM, normal appearing white matter; BBB, blood brain barrier; IFN-γ, interferon γ; TNF-α, tumor necrosis factor-α; RR, relapsing-remitting; MRI, magnetic resonance imaging; 3D, 3-dimensional; FLAIR, fluid-attenuated inversion recovery; EDSS, Expanded Disability Status Scale; IgG, immunoglobulin G; DVR, distribution volume ratio; ANCOVA, analysis of covariance; DMT, disease modifying treatment; ARR, annualized relapse rate; IgM, immunoglobulin M.

* Corresponding author at: Turku PET Centre, Turku University Hospital and University of Turku, Po Box 52, 20521 Turku, Finland.
E-mail address: sjkorp@utu.fi (S. Laaksonen).

https://doi.org/10.1016/j.msard.2023.104755
Received 11 December 2022; Received in revised form 24 April 2023; Accepted 8 May 2023
Available online 10 May 2023

blood-brain barrier (BBB) and once within the CNS, T cells start to release pro-inflammatory cytokines such as interferon γ (IFN-γ), which activate the brain-resident microglia. Activated microglia secrete chemokines, reactive oxygen species and pro-inflammatory cytokines and potentiate the inflammatory reaction within the CNS (Mallucci et al., 2015). Activated microglia are found widespread in the NAWM, and in association with various MS lesion types, such as acute lesions and chronic active lesions during the entire MS disease course (Kamma et al., 2022; O'Loughlin et al., 2018). The factors driving the persistent chronic microglial activation found in MS are currently not well understood, but potential candidates include the accumulation of iron in extracellular space after demyelination and death of oligodendrocytes, and meningeal inflammation leading to production of IFN-γ and tumor necrosis factor-α (TNF-α). In addition, fibrin, converted from blood derived fibrinogen, can activate microglia (Kamma et al., 2022).

In this study, we explored associations between early disease-related clinical and paraclinical parameters and later TSPO-PET-measurable innate immune cell activation in a cohort of patients with relapsing-remitting (RR) MS.

2. Material and methods

2.1. Study design/procedures

The study design is presented in Fig. 1. Study protocol included concurrent PET-imaging using TSPO-[^{11}C]PK11195 to evaluate microglial activation, 3T MRI and clinical evaluation for disability using Expanded Disability Status Scale (EDSS). In addition, medical records were reviewed retrospectively for relevant disease-related parameters.

2.2. Study participants

The study participants were recruited from the outpatient clinic of the Division of Clinical Neurosciences at the University Hospital of Turku, Finland during 2013-2018. The cohort consisted of 37 patients with RRMS (32 females). Inclusion criteria included at least 5 years disease duration, age 40-55 years and RR disease course at the time of enrolment. Exclusion criteria included clinical relapse and/or corticosteroid treatment within 30 days of evaluation, gadolinium contrast enhancement in magnetic resonance imaging (MRI), active neurological or autoimmune disease other than MS, another notable comorbidity, pregnancy and intolerability to PET or MRI. A group of 14 healthy age-matched control participants was imaged for comparison. The study protocol was approved by the Ethical Committee of the Hospital District of Southwest Finland. A written informed consent form was obtained from all participants. The study was conducted according to the principles of the Declaration of Helsinki.

2.3. Retrospectively obtained data

Medical records were reviewed retrospectively for relevant disease-related clinical and paraclinical parameters (Table 1), including number of T2 lesions in diagnostic MRI, immunoglobulin G (IgG) index in diagnostic CSF sample, and EDSS scores at various time points before PET-imaging. The quantity of T2 lesions was extracted from original MRI reports. Where possible (n = 27, 75 %), an experienced neuroradiologist re-evaluated the original diagnostic MR-images for an exact number of T2 lesions. Original MR-images were not available for all patients and image quality was not sufficient in some cases. In these cases (n = 9), estimation of T2 lesion number was based on the written neuroradiologist report and patients were categorized to the most probable of three subgroups (<10, 10-20 or >20 lesions).

2.4. [^{11}C]PK11195 production and image acquisition

The radiochemical synthesis of [^{11}C]PK11195 was performed as described previously (Rissanen et al., 2018, 2014). The mean injected dose was 489 ± 13 MBq (mean ± SD) for patients with MS and 487 ± 17 MBq for the HCs, with no difference between the groups.

PET was performed with a brain dedicated ECAT High-Resolution Research Tomograph scanner (CTI/Siemens) with an intrinsic spatial resolution of approximately 2.5 mm. First, a 6-min transmission scan for attenuation correction was obtained using a ^{137}Cs point source, and then a 60-min dynamic imaging was started simultaneously with the intravenous bolus injection of the [^{11}C]PK11195. A thermoplastic mask was used to minimize head movements. For anatomic reference, MRI was obtained using a 3T Ingenuity TF PET/MR scanner (Philips Healthcare) including 3-dimensional (3D) fluid-attenuated inversion recovery (FLAIR), 3D-T1, and 3D-T1 with gadolinium enhancement sequences (slice thickness 1 mm, FOV=256 × 256 mm, spatial resolution 1 × 1 × 1

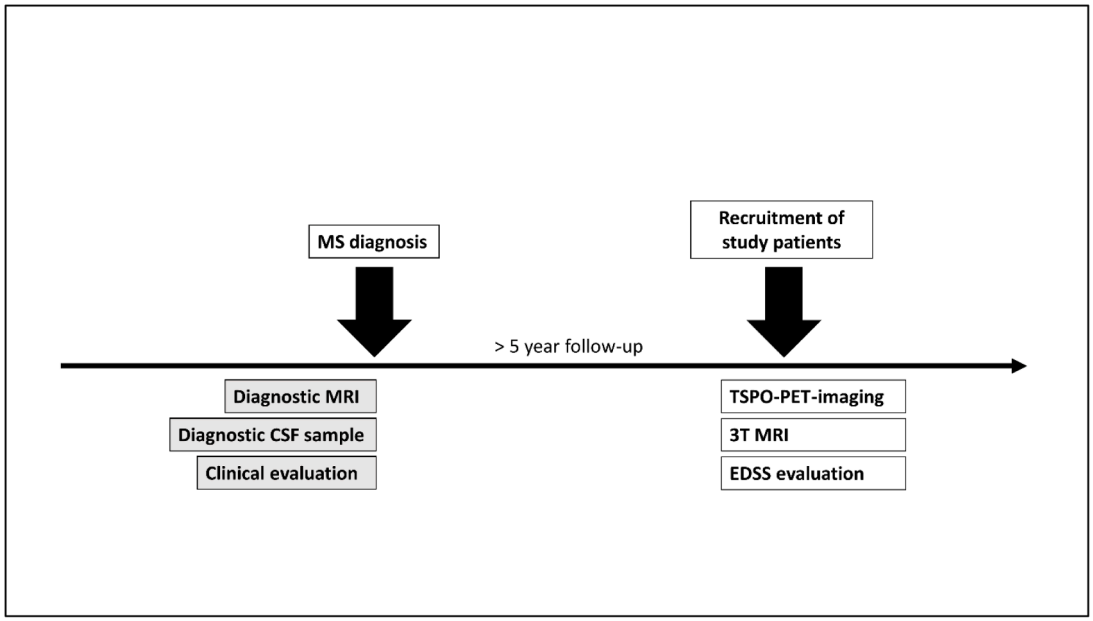

Fig. 1. Study design. This study explored which early clinical and paraclinical parameters would associate with later TSPO-PET measurable microglial activation.

Table 1
Retrospectively inspected parameters.

		Missing data
Age at diagnosis, mean (SD)	35.7 (5.9)	-
EDSS at diagnosis	1.5 (1–2)	7 (19 %)
EDSS at 5 years after diagnosis	2 (1–2.5)	8 (22 %)
Relapse characteristics		
Type of first symptoms		4 (11 %)
Optic neuritis	10 (30 %)	
Spinal onset	7 (21 %)	
Supratentorial onset	4 (12 %)	
Infratentorial onset	12 (36 %)	
Motor, cerebellar or bladder/bowel onset	17 (46 %)	-
Multifocal onset	10 (27 %)	-
Fully recovered from first relapse	18 (51 %)	2 (5 %)
Number of relapses 0-2 years after diagnosis	2 (1–3)	-
Time between 1st and 2nd relapse at most 2 years	27 (79 %)	3 (8 %)
CSF findings at diagnosis		
IgG index	0.81 (0.61–1.27)	2 (5 %)
MRI findings at diagnosis		
Gadolinium enhancement at diagnosis	15 (47 %)	5 (14 %)
Number of T2 lesions at diagnosis	10 (6-18)	9 (24 %)
Grouped number of T2 lesions at diagnosis		1 (3 %)
<10	14 (39 %)	
10–20	16 (44 %)	
>20	6 (17 %)	
Treatment initiation		
Time from diagnosis to treatment (days)	64.0 (28.5–375)	1 (3 %)
Time from first symptoms to treatment (days)	536 (240–1399)	1 (3 %)
DMT initiation within 3 years from diagnosis	32 (87 %)	-

Data was collected from medical records retrospectively. Continuous variables are presented as median (IQR) and categorical variables as number of patients (%), unless otherwise mentioned. CSF = cerebral spinal fluid, DMT = disease modifying treatment, EDSS = Expanded Disability Status Scale, IgG = immunoglobulin G.

mm, acquisition matrix 256 × 256 mm). For most of the patients (n=32, 86 %), MRI and PET were performed on the same day. For four patients, the time gap between PET and MRI was 1-8 days and in one patient, the time gap was somewhat longer (32 days).

2.5. PET post-processing and analysis

PET-images were reconstructed using 17-time frames and the dynamic data were then smoothed using a Gaussian 2.5-mm post-reconstruction filter as described previously (Rissanen et al., 2018, 2014). Possible displacements between frames were corrected using mutual information realignment in SPM8. Finally, all images were co-registered with concurrent T1 MRI.

Regions of interest (ROI) masks for T2 hyperintense and T1 hypointense lesions were created based on MR-images performed concurrently with TSPO-PET. A semi-automated method by the Lesion Segmentation Tool (Schmidt et al., 2012) with manual slice by slice correction was used as described previously (Rissanen et al., 2018). Freesurfer 5.3 software was used for segmenting cortical grey matter (GM), white matter (WM) and thalamus as previously reported (Rissanen et al., 2014). The NAWM ROI was created by removing the T2 lesion ROI from the WM ROI. The perilesional ROI was created by dilating the corresponding T1 lesion ROI mask by six voxels and then removing the core and 3-voxel area surrounding the core from it.

Microglial activation was evaluated as specific binding of [^{11}C] PK11195 using distribution volume ratio (DVR) in prespecified ROIs: NAWM, T1 lesions, T2 lesions, perilesional NAWM, cortical GM and thalamus. To reduce the partial volume effects from cortex and ventricles, 1 mm area was eroded from NAWM ROI at the borders of cortical and subcortical GM, and periventricular area. DVRs were estimated as previously described (Rissanen et al., 2018).

2.6. Statistical analysis

The statistical analyses were performed using R (version 4.1.1). Variables are reported as mean ± SD unless otherwise stated. For all analyses a p-value < 0.05 was considered statistically significant.

Associations between each variable (Table 1) and DVR values of prespecified ROIs were analyzed. Wilcoxon rank-sum test was used in initial comparisons between categorical variables and DVRs. Holm adjustment was used for p-values, if more than two groups were compared. Spearman correlations were used to assess such relationships regarding the ordinal and continuous variables.

Patients were classified into subgroups according to the number of T2 lesions in the diagnostic MRI (<10, 10-20 and >20 lesions) and EDSS at five years after diagnosis (<2.0 and ≥2.0). EDSS score 2.0 was chosen to represent early disability accumulation as it is the first EDSS score indicating disability in one functional area, whereas EDSS scores <2.0 point out that only abnormal signs not leading to disability are observed in neurological examination.

To adjust the results for confounding factors, multiple linear regression model was used for continuous variables of interest and analysis of covariance (ANCOVA) was used for categorical variables of interest. Used covariates were time until treatment initiation (≥3 years or <3 years from diagnosis), treatment before imaging, age at imaging, disease duration (from diagnosis) at imaging and sex. As there was only one patient without treatment, treatment before imaging was categorized into two groups: no treatment or moderate-efficacy (interferons, glatiramer acetate, teriflunomide, dimethyl fumarate, fingolimod) and high-efficacy treatment (natalizumab) (Scolding et al., 2015). In pairwise comparisons (ANCOVA, multiple linear regression model), the p-values were adjusted using Tukey's method.

2.7. Data availability

Anonymized data not published within the article will be shared over the next three years upon a request from a qualified investigator.

3. Results

3.1. Demographic and clinical characteristics of participants

The study cohort included 37 RRMS-patients and 14 healthy controls (age 47.8 ± 3.8 vs. 45.8 ± 6.8 years, respectively, $p = 0.15$). The MS-cohort had 12.2 ± 5 years disease duration and 2.8 ± 0.8 EDSS at the time of PET-imaging (Table 2). Median time from first symptoms to diagnostic MRI was 167 days (range 0-4489 days) and from diagnostic MRI to PET-imaging 13.2 years (range 5.6-25.6 years). All except one MS-patient had used disease-modifying treatment (DMT) prior to PET-imaging. Thirteen patients (35 %) had used more than one DMT. Patients had used mainly moderate-efficacy DMTs and only four patients (11 %) had used high-efficacy DMT (natalizumab) (Table 2). Natalizumab-treated patients had a higher median annualized relapse rate (ARR) during the time period between disease onset and PET-imaging compared to patients who had not used high-efficacy treatment (0.51 vs. 0.30, $p = 0.029$), but otherwise there were no differences in the retrospectively inspected parameters or demographic factors. Patients had been on average 31 % of the follow-up period on natalizumab treatment. The DVR values reflecting TSPO-binding and microglial activation were significantly higher in MS-patients compared to HCs in the NAWM and thalamus ($p = 0.039$ and $p = 0.017$, respectively), but not in cortical GM (Fig. 2). Patients who had used natalizumab prior to PET-imaging had a higher DVR in the perilesional NAWM (1.24 vs. 1.18, $p = 0.033$) and a lower DVR in the cortical GM (1.20 vs. 1.24, $p = 0.025$) compared to patients who had not used high-efficacy DMTs. In other studied ROIs there were no differences in the DVRs between these subgroups.

Table 2
Demographics of MS-cohort at PET-imaging (n = 37).

Age (years), mean (SD)	47.8 (3.8)
Disease duration (years), mean (SD)	12.2 (5)
Sex, female	32 (87 %)
Total number of relapses before imaging	5 (3–6)
ARR	0.32 (0.22–0.44)
On-treatment relapses[a]	25 (69 %)
EDSS	2.5 (2–3)
EDSS change from diagnosis to imaging[a]	1 (1–2)
MSSS	2.64 (1.80–4.13)
Time on any treatment (years)[a]	9.5 (5.9–13.2)
First DMT	
Interferon beta	29 (78 %)
Glatiramer acetate	5 (14 %)
Natalizumab	2 (5 %)
No treatment ever	1(3 %)
Used DMTs prior to PET imaging, number of patients	
Interferon beta	32 (86 %)
Glatiramer acetate	16 (43 %)
Teriflunomide	11 (30 %)
Dimethyl fumarate	5 (14 %)
Fingolimod	6 (16 %)
Natalizumab	4 (11 %)
No treatment ever	1 (3 %)
DMT at PET imaging	
Interferon beta	6 (16 %)
Glatiramer acetate	3 (8 %)
Teriflunomide	10 (27 %)
Dimethyl fumarate	2 (5 %)
Fingolimod	5 (14 %)
No treatment	11 (30 %)

Continuous variables are presented as median (IQR) and categorical variables as n (%), unless otherwise mentioned.
[a]Number of patients with missing data: on-treatment relapses 1 (3 %), EDSS change from diagnosis to imaging 7 (19 %), time on any treatment 1 (3 %).
ARR = annualized relapse rate, DMT = Disease modifying treatment, EDSS = Expanded Disability Status Scale, IQR = interquartile range, MSSS = Multiple Sclerosis Severity Score, PET = positron emission tomography, SD = standard deviation.

3.2. Number of T2 lesions at the time of diagnosis associates with later TSPO-[^{11}C]PK11195 uptake in the NAWM, perilesional NAWM, T1 lesions and thalamus

The median (interquartile range) number of T2 lesions per 27 original diagnostic MRI scan was 10 (6–18). Higher number of T2 lesions in diagnostic MRI correlated with higher DVR in perilesional NAWM (r = 0.4, p = 0.036), T1 lesions (r = 0.41, p = 0.029) and thalamus (r = 0.52, p = 0.004; Fig. 3).

When confounding factors were considered in multiple linear regression, higher number of T2 lesions in diagnostic MRI associated with later higher DVR in the NAWM (p = 0.020), in perilesional NAWM (p = 0.045) and in the thalamus (p = 0.006; Fig. 4) but the association between the number of T2 lesions and T1 lesion DVR was abrogated. T2 lesion DVR nor cortical GM DVR correlated with the number of T2 lesions, and no association was observed after multiple regression modelling either.

Patients (n = 36, 97 %) were then grouped according to the number of T2 lesions: <10 lesions (14 patients, 39 %), 10-20 lesions (16 patients, 41 %) or >20 lesions (6 patients, 17 %). In all studied ROIs except the cortical GM, the average DVRs were somewhat higher in patients with >20 lesions compared to patients with <10 lesions, although the difference reached statistical significance only in the thalamus (Table 3). However, when the confounding factors were considered in ANCOVA modelling, patients with >20 lesions had significantly higher DVR in the NAWM, perilesional NAWM and thalamus compared to the patients with <10 lesions (Fig. 5). Estimated differences between the groups were 0.066 in the NAWM (p = 0.006), 0.090 in perilesional NAWM (p = 0.011) and 0.117 in thalamus (p = 0.005). Similar results were observed for DVRs in the NAWM and the perilesional NAWM between patients with >20 lesions and patients with 10-20 lesions. Estimated differences between the groups were 0.064 in NAWM (p = 0.005) and 0.072 in perilesional NAWM (p = 0.041). Additionally, DVR in the thalamus was higher in the patients with 10-20 lesions compared to the patients with <10 lesions (estimated difference 0.063, p = 0.039; Fig. 5). T1 and T2 lesion DVRs and cortical GM DVR did not differ significantly between the different T2 lesion groups, when multiple comparison corrections and modelling with confounding factors were considered.

3.3. IgG index at the time of MS diagnosis associates with later TSPO-[^{11}C]PK11195 uptake in the NAWM

IgG index at diagnosis was available for 35 patients and was elevated (> 0.6) in 29 (83 %) patients. Higher IgG index correlated with higher DVR in the NAWM (r = 0.35, p = 0.039; Fig. 6). However, this association did not survive in multiple linear regression (regression estimate

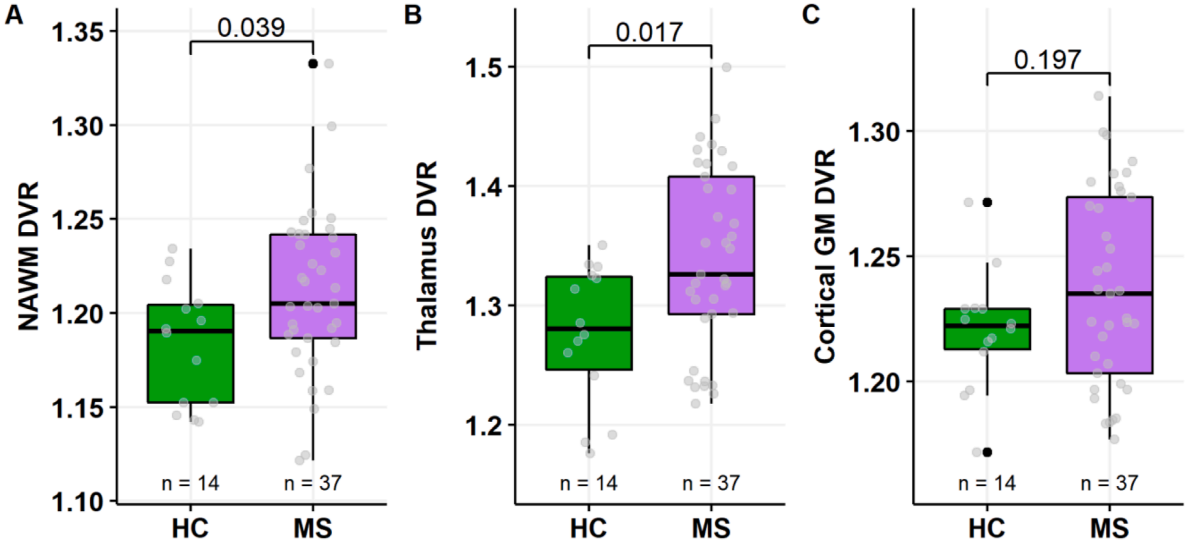

Fig. 2. TSPO-PET DVR values in MS-patients and healthy controls. MS-patients had significantly higher DVR in the NAWM (A), and thalamus (B) compared to healthy controls. The difference in cortical grey matter (C) was not statistically significant. Wilcoxon rank-sum test was used. DVR = distribution volume ratio, GM = grey matter, NAWM = normal appearing white matter.

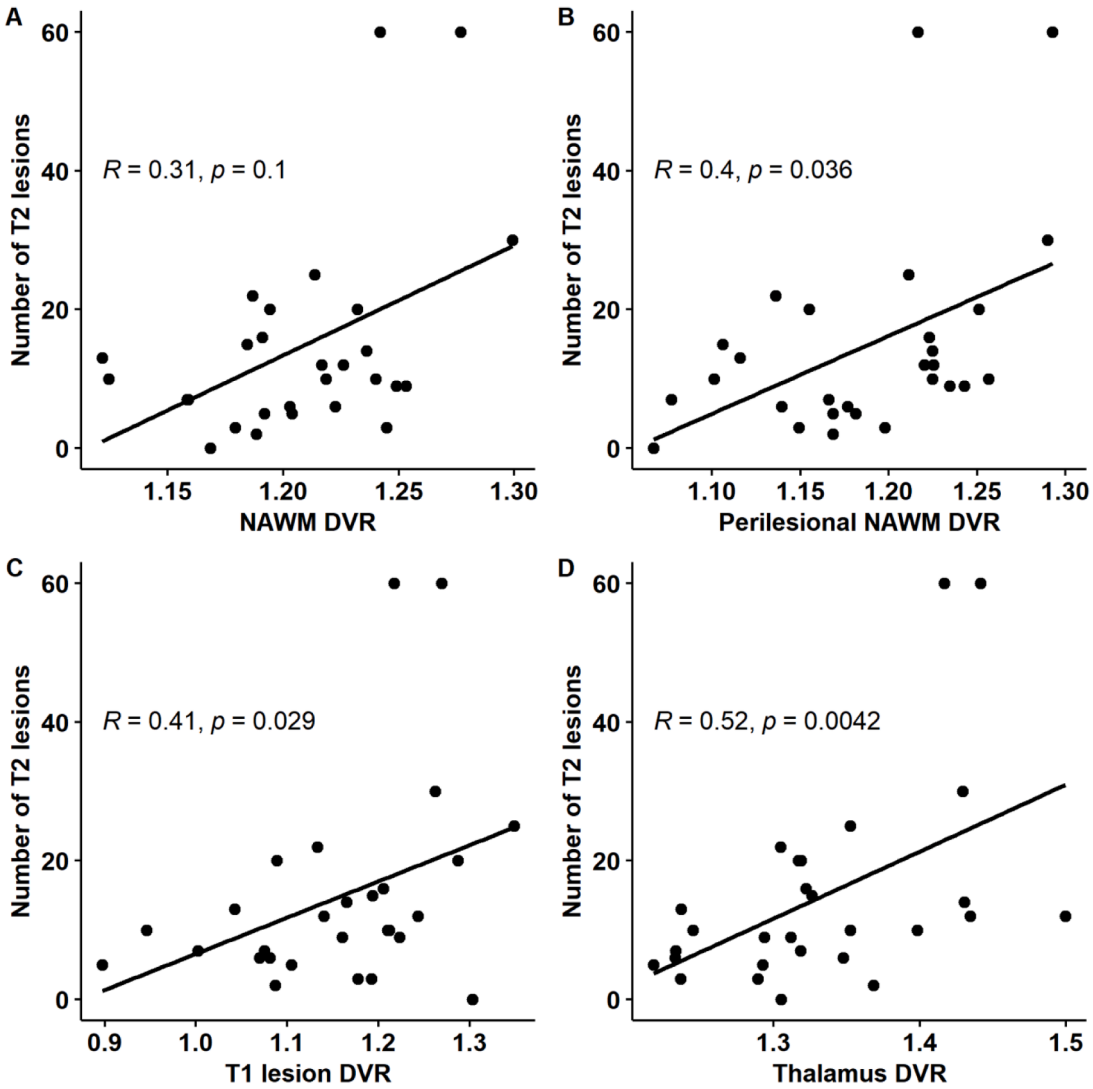

Fig. 3. Spearman correlations between the number of T2 lesions at diagnosis and later TSPO-PET DVR values (n = 27). In the entire NAWM (A) the correlation did not reach statistical significance while in the perilesional NAWM (B), T1 lesions (C) and thalamus (D) later microglial activation correlated with a higher number of T2 lesions at diagnosis. DVR*r*= distribution volume ratio in the TSPO-PET image obtained after follow-up, NAWM = normal appearing white matter, *r* = Spearman correlation coefficient.

0.033, $p = 0.057$). In other studied ROIs, no significant correlations with IgG index and DVRs were observed (data not shown).

3.4. Combined effect of IgG index and number of T2 lesions on TSPO-[^{11}C]PK11195 uptake in NAWM

The strength of IgG index as a predictor of later microglial activation in the NAWM was improved ($p = 0.048$), when both IgG index and the number of T2 lesions were added to the regression model with NAWM DVR as an outcome, along with the confounding factors. The effect of the number of T2 lesions remained significant ($p = 0.018$). Both variables were also significant when the categorized number of T2 lesions was added to the model with IgG index and the adjusting variables (Supplemental Table 1).

3.5. EDSS at 5 years after diagnosis associates with later TSPO-[^{11}C]PK11195 uptake in perilesional NAWM

Mean EDSS was 1.6 ± 1.3 at the time of diagnosis and 2.0 ± 1.2 at 5 years after diagnosis. Patients were divided into two groups according to the EDSS at 5 years after diagnosis. 13 patients had EDSS at most 1.5 (45 %) and 16 patients had EDSS ≥2.0 (55 %). DVR in the perilesional NAWM was higher in patients with EDSS ≥2.0 compared to the patients with lower EDSS (1.21 ± 0.07 vs. 1.16 ± 0.06; $p = 0.045$), and the difference remained significant after ANCOVA modelling ($p = 0.008$; Fig. 7). No significant difference in TSPO binding was observed in other studied ROIs between EDSS subgroups (data not shown).

4. Discussion

This TSPO-PET study indicated that a higher number of T2 lesions in MRI at the time of MS diagnosis associates with more pronounced microglial activation later during the disease in the NAWM, perilesional NAWM and thalamus. In addition, the magnitude of the IgG index measured at the time of MS diagnosis associated with later microglial activation in the NAWM. More abundant microglial activation was observed in patients with EDSS score ≥2.0 (indicating early disability accumulation) at five years after diagnosis compared to patients with a lower EDSS score. As increased microglial activation is known to associate with greater likelihood of later disease progression (Sucksdorff et al., 2020), our results demonstrate a potential link of early adaptive immune cell activity via microglial activation to later disease

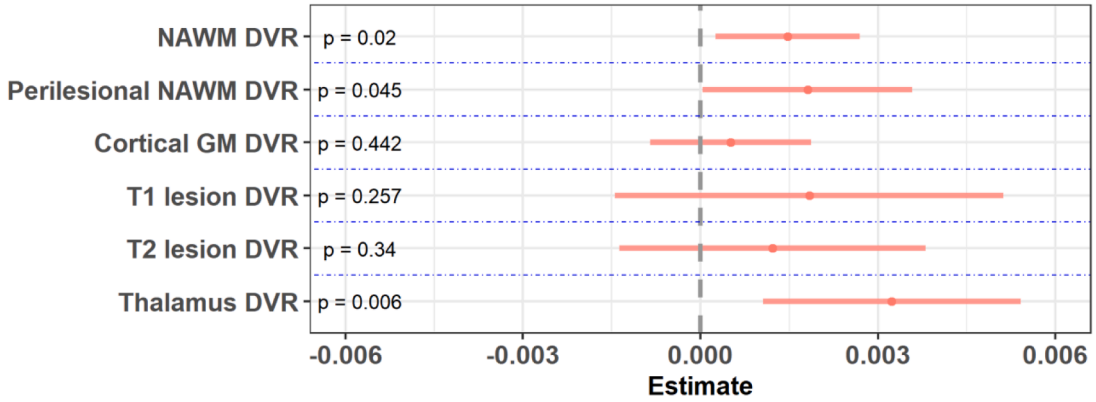

Fig. 4. The effect of the number of T2 lesions on regional brain DVR values according to a multiple linear regression model. Higher number of T2 lesions in diagnostic MRI associated with later higher DVR value in the NAWM (regression estimate 0.0015 indicates that NAWM DVR increases 0.0015 units per one additional T2 lesion), in perilesional NAWM (regression estimate 0.0018) and in the thalamus (regression estimate 0.0032). The red dots represent the regression estimates and red lines represent the confidence intervals. Time until treatment initiation (≥3 years or <3 years from diagnosis), treatment before PET-imaging (no/moderate-efficacy treatment or high-efficacy treatment), age and disease duration at PET-imaging, and sex were used as covariates in the multiple linear regression model. DVR = distribution volume ratio, GM = grey matter, NAWM = normal appearing white matter. (For interpretation of the references to colour in this figure legend, the reader is referred to the web version of this article.)

Table 3
Average DVR values of MS-patients grouped according to number of T2 lesions and in healthy controls.

Region of interest	Number of T2 lesions			p-value			HC	p-value		
	<10	10–20	>20	<10 vs. 10-20	<10 vs. >20	10–20 vs. >20		HC vs. <10	HC vs. 10–20	HC vs. >20
NAWM	1.20 (0.03)	1.20 (0.04)	1.26 (0.05)	0.8	0.051	0.059	1.18 (0.03)	0.17	0.088	0.012*
Perilesional NAWM	1.17 (0.05)	1.19 (0.05)	1.25 (0.08)	0.3	0.053	0.2	-	-	-	-
T1 lesions	1.13 (0.11)	1.15 (0.09)	1.24 (0.07)	0.5	0.032	0.021	-	-	-	-
T2 lesions	1.14 (0.09)	1.15 (0.09)	1.22 (0.06)	0.6	0.041	0.049	-	-	-	-
Cortical GM	1.24 (0.03)	1.23 (0.04)	1.25 (0.05)	0.5	0.8	0.4	1.22 (0.02)	0.2	0.5	0.5
Thalamus	1.29 (0.06)	1.36 (0.08)	1.39 (0.05)	0.009*	0.005*	0.4	1.28 (0.06)	0.8	0.011*	0.003*

*= remains statistically significant at a level of $p < 0.05$ (Wilcoxon rank-sum test) after Holm adjustment for multiple (n = 3) comparisons.
The variables are presented as mean (SD). DVR = distribution volume ratio, GM = grey matter, HC = healthy control, NAWM = normal appearing white matter, SD = standard deviation

progression. This comprises both focal acute (T2 lesions) and diffuse and more chronic (intrathecal IgG production) adaptive immune cell activation. Our study suggests that adaptive immune system activation is an important driver of the persistent proinflammatory innate immune system phenotype in brain (Dendrou et al., 2015; Ransohoff et al., 2015).

Increased TSPO-PET-measurable microglial activation in MS brain is perceived as an undesirable phenomenon. Several studies indicate that TSPO-PET signal increases with advancing MS disease (Debruyne et al., 2003; Rissanen et al., 2014; Sucksdorff et al., 2020). Increased TSPO-binding predicts later disease progression (Sucksdorff et al., 2020). Microglial/macrophage activation is potentially detrimental already early during the disease course, as higher TSPO-binding at clinically isolated syndrome increased the subsequent risk of clinically definite MS during a 2-year follow-up (Giannetti et al., 2015).

Thalamus-related pathology has been observed to predict progression in MS (Azevedo et al., 2018; Magon et al., 2020). This may be partially driven by pathology in those white matter tracts that lead to the respective areas of the thalamus (Banati et al., 2000; Herranz et al., 2016; Rissanen et al., 2014; Sucksdorff et al., 2020). In our study, abundant focal inflammation in early disease was associated with later higher thalamic DVR values. Recently we showed that thalamic microglial activation is a predictor of later MS disease progression (Misin et al., 2022). Hence, our results are in line with previous studies associating thalamic atrophy and microglial activation with later disease progression.

The association between early high T2 lesion burden and later prominent microglial activation observed here was not entirely unexpected. T2 lesion burden in early disease has been shown to correlate with higher probability of later disability development and conversion to progressive disease (Fisniku et al., 2008; Uher et al., 2017). Large real-life register studies demonstrate that high-efficacy treatment, particularly when initiated soon after MS diagnosis prevents later disease progression (Bergamaschi et al., 2016; Brown et al., 2019; Iaffaldano et al., 2021). We can hypothesize that efficient treatments, which block the adaptive immune cell entry into the CNS, reduce the overall inflammatory burden and innate immune cell activation, and might thereby delay or even prevent progression.

Our results suggest that elevated IgG index at diagnosis might have an impact on later disease course, as more widespread microglial activation associated with higher IgG index. Interestingly, recent studies suggest that CSF factors, such as IgG, may drive microglial activation (Fadda et al., 2019). Our observation of the association of a high CSF IgG index with increased microglial activation in the NAWM surrounding ventricles is in line with this (Mahajan et al., 2020). Increased production of intrathecal immunoglobulin by plasma cells, as well as high T2 lesion number, may reflect high early diffuse inflammatory burden. Instead of residing (solely) in the acute focal white matter lesions, plasma cells likely represent more diffuse CNS inflammation for example in meninges and perivascular spaces. Predictive value of IgG index in MS progression is controversial, as in some, but not all, studies higher IgG index has been associated with SPMS conversion (Izquierdo G et al., 2002). CSF immunoglobulin M (IgM) concentration might be a better biomarker than IgG for active inflammatory process in MS (Mailand and

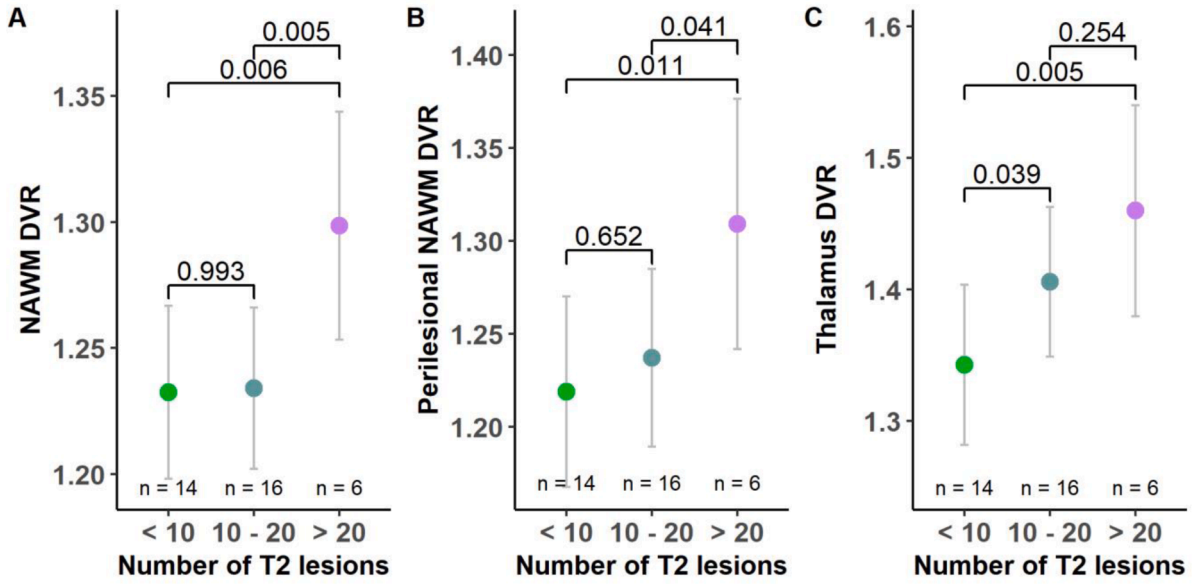

Fig. 5. The estimated means of DVR values in NAWM, perilesional NAWM and thalamus according to the number of T2 lesions at diagnosis. In the NAWM (A) and perilesional NAWM (B), the group with >20 lesions had significantly higher DVR values compared to the group with 10–20 and <10 lesions. In thalamus (C), the group with 10–20 lesions and >20 lesions had significantly higher DVR values compared to the group with <10 lesions. ANCOVA was used in the modelling and time until treatment initiation (≥3 years or <3 years from diagnosis), treatment before PET-imaging (no/moderate-efficacy treatment or high-efficacy treatment), age and disease duration at PET-imaging and sex were used as covariates. ANCOVA = analysis of covariance, DVR = distribution volume ratio, NAWM = normal appearing white matter.

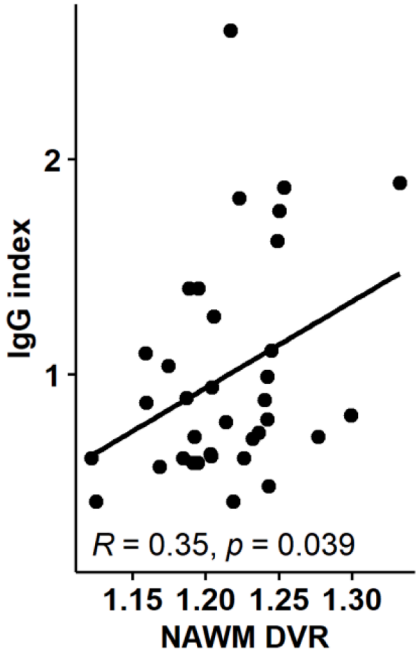

Fig. 6. Spearman correlation between IgG index and later DVR value in the NAWM. Higher IgG index in the diagnostic CSF sample correlated with a higher DVR value in the NAWM in a TSPO-PET image obtained after follow-up. DVR = distribution volume ratio, IgG = immunoglobulin G, NAWM = normal appearing white matter, *r* = Spearman correlation coefficient.

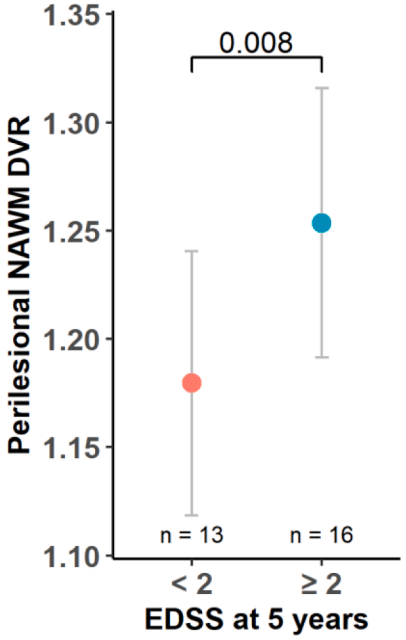

Fig. 7. The estimated means of DVR values in perilesional NAWM according to EDSS values 5 years from diagnosis. DVR values in the perilesional NAWM were higher in patients with EDSS at least 2.0 compared to the patients with EDSS less than 2.0. ANCOVA was used in the modelling, and time until treatment initiation (≥3 years or <3 years from diagnosis), treatment before PET-imaging (no/moderate-efficacy treatment or high-efficacy treatment), age and disease duration at PET-imaging, and sex were used as covariates. ANCOVA = analysis of covariance, DVR = distribution volume ratio, EDSS = Expanded Disability Status Scale, NAWM = normal appearing white matter.

Frederiksen, 2020). Unfortunately, data about IgM concentrations was not available for patients included in the present study.

In previous large epidemiological studies, early disability accumulation, male sex, older age at diagnosis, relapse characteristics and relapse rate have predicted more severe disease course (Confavreux and Vukusic, 2006; Scalfari et al., 2014; Tremlett et al., 2008). Similarly, in our study a higher EDSS at 5 years after diagnosis associated with more pronounced microglial activation later during disease in perilesional NAWM, which has been linked in our earlier study to disease

progression (Sucksdorff et al., 2020).

Our study has some limitations. Information on potential prognosticators were obtained from medical records and the unavoidable missing data may have weakened the statistical power of certain analyses. The quality and resolution of the diagnostic MRI scans varied depending on MRI camera.Exact number of T2 lesions was calculated from the diagnostic MRI scans, which were not available for all patients. In nine patients, the number of T2 lesions was estimated from neuroradiology reports to classify patients to T2 lesion subgroups. The possible difference between counted and estimated T2 numbers might have influenced the results presented in Fig. 5. However, similar results were obtained in other analyses, where exact numbers of T2 lesions were used. In addition, sizes of individual lesions or total lesion load at the time of diagnosis could not be considered as a potential prognosticator, although there can be wide variation in the size of lesions. We used the first generation TSPO-ligand [^{11}C]PK11195 for assessment of smouldering inflammation. This ligand has limitations such as limited affinity to the target compared to second-generation TSPO-ligands. The benefits of using this ligand, however, include a well-validated post-processing and image analysis methods, no necessity of patient genotyping for ligand binding affinity evaluation, and substantial clinical imaging experience in MS (Giannetti et al., 2014; Politis et al., 2012; Rissanen et al., 2018, 2014; Sucksdorff et al., 2019; Turkheimer et al., 2007). In addition, it is important to consider the possible partial volume effect especially in small or narrow ROIs such as cortical GM.

The inclusion of study participants was limited by age and disease duration to obtain a clinically homogenous cohort of late stage RRMS-patients with potential variability in CNS glial pathology. However, as the study population represents a real-life cohort, most patients were using or had used various DMTs. We cannot exclude the possible effect of heterogeneous DMTs on innate immune cell activation, but this aspect and other possible confounding factors were carefully taken into account in our analyses and in interpretation of the results (Scalfari et al., 2014; Tremlett et al., 2008; Uher et al., 2017).

5. Conclusions

In summary, our results highlight the importance of early inflammatory events in development of later progression-related pathology. We plan to continue the follow-up of the present cohort to evaluate their later disease course (NCT03134716, ClinicalTrials.gov). Several register-based studies highlight the importance of early initiation of high-efficacy DMTs (Brown et al., 2019; Harding et al., 2019; Iaffaldano et al., 2021) which prevent relapses and focal MRI activity efficiently. According to our study, especially patients with high IgG index and T2 lesion burden at diagnosis should be treated early and effectively, to prevent later microglial activation and disease progression. Until better, CNS pathology-targeting treatments are available, we strongly recommend the early effective treatment principle for the long-term benefit of MS-patients.

Author contributions

Sini Laaksonen: conceptualization; investigation; resources; data curation; writing – original draft (lead); writing – review and editing

Maija Saraste: conceptualization; study design; writing – original draft (supporting); writing – review and editing

Marcus Sucksdorff: conceptualization; study design; writing – review and editing

Marjo Nylund: investigation; resources; writing – review and editing

Anna Vuorimaa: investigation; writing – review and editing

Markus Matilainen: methodology (lead); formal analysis (lead); data curation; writing – review and editing

Jaakko Heikkinen: investigation; writing – review and editing

Laura Airas: conceptualization; methodology (supporting); writing original draft (supporting); writing – review and editing supervision; supervision; funding acquisition

S.L., M. Sa., M. Su. and L. A. contributed to the study conception and design. Material preparation, data collection and analysis were performed by S.L., M. Sa., M. Su., M. N., A. V., J. H. and L. A. Biostatical analyses were performed by M. M. The first draft of the manuscript was written by S. L. and all authors commented on previous versions of the manuscript. All authors read and approved the final manuscript.

Funding

This work was supported by the Academy of Finland grant for clinical researcher [330902]; Sigrid Juselius Foundation, and the InFLAMES Flagship Programme of the Academy of Finland [337530].

Declaration of Competing Interest

M.Sa., M.M., M.N. and J.H. have no competing interests. S.L. has received travel honoria from Roche, and research support from Turunmaa Duodecim society, Finnish Brain Foundation and Turku Doctoral Programme in Clinical Research. M.Su. has served on advisory boards for Sanofi-Aventis and Roche and has received speaker honoraria from Merck Serono and travel honoraria from Orion, Roche, Biogen and Sanofi-Aventis and received research support from The Finnish Medical Foundation, The Finnish MS Foundation and from The Finnish Medical Society (Finska Läkaresällskapet). A.V. has received speaker honoraria from Janssen. L.A. has received honoraria from Biogen, Roche, Genzyme, Merck Serono and Novartis, and institutional research grant support from Finnish Academy, Sanofi-Genzyme, and Merck Serono.

Acknowledgements

We thank all multiple sclerosis patients participating in this study, and the expert personnel of the Turku PET Centre making this study possible. Dr. Jouni Tuisku is acknowledged for expert advice regarding the PET processing.

Supplementary materials

Supplementary material associated with this article can be found, in the online version, at doi:10.1016/j.msard.2023.104755.

References

Azevedo, C.J., Cen, S.Y., Khadka, S., Liu, S., Kornak, J., Shi, Y., Zheng, L., Hauser, S.L., Pelletier, D., 2018. Thalamic atrophy in multiple sclerosis: a magnetic resonance imaging marker of neurodegeneration throughout disease. Ann. Neurol. 83, 223–234. https://doi.org/10.1002/ANA.25150.

Banati, R.B., Newcombe, J., Gunn, R.N., Cagnin, A., Turkheimer, F., Heppner, F., Price, G., Wegner, F., Giovannoni, G., Miller, D.H., Perkin, G.D., Smith, T., Hewson, A.K., Bydder, G., Kreutzberg, G.W., Jones, T., Cuzner, M.L., Myers, R., 2000. The peripheral benzodiazepine binding site in the brain in multiple sclerosis. Quantitative *in vivo* imaging of microglia as a measure of disease activity. Brain 123, 2321–2337. https://doi.org/10.1093/brain/123.11.2321.

Bergamaschi, R., Quaglini, S., Tavazzi, E., Amato, M.P., Paolicelli, D., Zipoli, V., Romani, A., Tortorella, C., Portaccio, E., D'Onghia, M., Garberi, F., Bargiggia, V., Trojano, M., 2016. Immunomodulatory therapies delay disease progression in multiple sclerosis. Mult. Scler. 22, 1732–1740. https://doi.org/10.1177/1352458512445941.

Brown, J.W.L., Coles, A., Horakova, D., Havrdova, E., Izquierdo, G., Prat, A., Girard, M., Duquette, P., Trojano, M., Lugaresi, A., Bergamaschi, R., Grammond, P., Alroughani, R., Hupperts, R., McCombe, P., van Pesch, V., Sola, P., Ferraro, D., Grand'Maison, F., Terzi, M., Lechner-Scott, J., Flechter, S., Slee, M., Shaygannejad, V., Pucci, E., Granella, F., Jokubaitis, V., Willis, M., Rice, C., Scolding, N., Wilkins, A., Pearson, O.R., Ziemssen, T., Hutchinson, M., Harding, K., Jones, J., McGuigan, C., Butzkueven, H., Kalincik, T., Robertson, N., 2019. Association of initial disease-modifying therapy with later conversion to secondary progressive multiple sclerosis. JAMA - J. Am. Med. Assoc. 321, 175–187. https://doi.org/10.1001/jama.2018.20588.

Confavreux, C., Vukusic, S., 2006. Age at disability milestones in multiple sclerosis. Brain 129, 595–605. https://doi.org/10.1093/brain/awh714.

Debruyne, J.C., Versijpt, J., van Laere, K.J., de Vos, F., Keppens, J., Strijckmans, K., Achten, E., Slegers, G., Dierckx, R.A., Korf, J., de Reuck, J.L., 2003. Pet visualization

of microglia in multiple sclerosis patients using [11C]PK11195. Eur. J. Neurol. 10, 257–264. https://doi.org/10.1046/j.1468-1331.2003.00571.x.
Dendrou, C.A., Fugger, L., Friese, M.A., 2015. Immunopathology of multiple sclerosis. Nat. Rev. Immunol. 15, 545–558. https://doi.org/10.1038/NRI3871.
Fadda, G., Brown, R.A., Magliozzi, R., Aubert-Broche, B., O'Mahony, J., Shinohara, R.T., Banwell, B., Marrie, R.A., Yeh, E.A., Collins, D.L., Arnold, D.L., Bar-Or, A., 2019. A surface-in gradient of thalamic damage evolves in pediatric multiple sclerosis. Ann. Neurol. 85, 340–351. https://doi.org/10.1002/ANA.25429.
Fisniku, L.K., Brex, P.A., Altmann, D.R., Miszkiel, K.A., Benton, C.E., Lanyon, R., Thompson, A.J., Miller, D.H., 2008. Disability and T2 MRI lesions: a 20-year follow-up of patients with relapse onset of multiple sclerosis. Brain 131, 808–817. https://doi.org/10.1093/brain/awm329.
Frischer, J.M., Weigand, S.D., Guo, Y., Kale, N., Parisi, J.E., Pirko, I., Mandrekar, J., Bramow, S., Metz, I., Brück, W., Lassmann, H., Lucchinetti, C.F., 2015. Clinical and pathological insights into the dynamic nature of the white matter multiple sclerosis plaque. Ann. Neurol. 78, 710–721. https://doi.org/10.1002/ana.24497.
Giannetti, P., Politis, M., Su, P., Turkheimer, F., Malik, O., Keihaninejad, S., Wu, K., Reynolds, R., Nicholas, R., Piccini, P., 2014. Microglia activation in multiple sclerosis black holes predicts outcome in progressive patients: An *in vivo* [(11)C](R)-PK11195-PET pilot study. Neurobiol. Dis. https://doi.org/10.1016/j.nbd.2014.01.018.
Giannetti, P., Politis, M., Su, P., Turkheimer, F.E., Malik, O., Keihaninejad, S., Wu, K., Waldman, A., Reynolds, R., Nicholas, R., Piccini, P., 2015. Increased PK11195-PET binding in normal-appearing white matter in clinically isolated syndrome. Brain 138, 110–119. https://doi.org/10.1093/brain/awu331.
Harding, K., Williams, O., Willis, M., Hrastelj, J., Rimmer, A., Joseph, F., Tomassini, V., Wardle, M., Pickersgill, T., Robertson, N., Tallantyre, E., 2019. Clinical outcomes of escalation vs early intensive disease-modifying therapy in patients with multiple sclerosis. JAMA Neurol. 76, 536–541. https://doi.org/10.1001/jamaneurol.2018.4905.
Herranz, E., Gianni, C., Louapre, C., Treaba, C.A., Govindarajan, S.T., Ouellette, R., Loggia, M.L., Sloane, J.A., Madigan, N., Izquierdo-Garcia, D., Ward, N., Mangeat, G., Granberg, T., Klawiter, E.C., Catana, C., Hooker Jacob, M., Taylor, N., Ionete, C., Kinkel, R., Mainero, C., 2016. The neuroinflammatory component of gray matter pathology in multiple sclerosis. Ann. Neurol. 80, 776–790. https://doi.org/10.1002/ana.24791.The.
Iaffaldano, P., Lucisano, G., Butzkueven, H., Hillert, J., Hyde, R., Koch-henriksen, N., Magyari, M., Pellegrini, F., Spelman, T., 2021. Early treatment delays long-term disability accrual in RRMS : results from the BMSD network. Multiple Sclerosis J. 1–13. https://doi.org/10.1177/13524585211010128.
Izquierdo, G, Angulo, S, Garcia-Moreno, JM, Gamero, MA, Navarro, G, Gata, JM, Ruiz-Pena, JL, Páramo, MD, 2002. Intrathecal IgG synthesis: marker of progression in multiple sclerosis patients. Acta Neurol. Scand. 105, 158–163.
Kamma, E., Lasisi, W., Libner, C., Ng, H.S., Plemel, J.R., 2022. Central nervous system macrophages in progressive multiple sclerosis: relationship to neurodegeneration and therapeutics. J. Neuroinflammation. https://doi.org/10.1186/s12974-022-02408-y.
Lassmann, H., 2018. Pathogenic mechanisms associated with different clinical courses of multiple sclerosis. Front. Immunol. 9, 3116. https://doi.org/10.3389/fimmu.2018.03116.
Luchetti, S., Fransen, N.L., van Eden, C.G., Ramaglia, V., Mason, M., Huitinga, I., 2018. Progressive multiple sclerosis patients show substantial lesion activity that correlates with clinical disease severity and sex: a retrospective autopsy cohort analysis. Acta Neuropathol. 135, 511–528. https://doi.org/10.1007/s00401-018-1818-y.
Magon, S., Tsagkas, C., Gaetano, L., Patel, R., Naegelin, Y., Amann, M., Parmar, K., Papadopoulou, A., Wuerfel, J., Stippich, C., Kappos, L., Chakravarty, M.M., Sprenger, T., 2020. Volume loss in the deep gray matter and thalamic subnuclei: a longitudinal study on disability progression in multiple sclerosis. J. Neurol. 267, 1536–1546. https://doi.org/10.1007/s00415-020-09740-4.
Mahajan, K.R., Nakamura, K., Cohen, J.A., Trapp, B.D., Ontaneda, D., 2020. Intrinsic and extrinsic mechanisms of thalamic pathology in multiple sclerosis. Ann. Neurol. 88, 81–92. https://doi.org/10.1002/ANA.25743.
Mailand, M.T., Frederiksen, J.L., 2020. Intrathecal IgM as a prognostic marker in multiple sclerosis. Mol. Diagn. Ther. 24, 263–277. https://doi.org/10.1007/S40291-020-00455-W.
Mallucci, G., Peruzzotti-Jametti, L., Bernstock, J.D., Pluchino, S., 2015. The role of immune cells, glia and neurons in white and gray matter pathology in multiple sclerosis. Prog. Neurobiol. 1. https://doi.org/10.1016/J.PNEUROBIO.2015.02.003, 0.
Misin, O., Matilainen, M., Nylund, M., Honkonen, E., Rissanen, E., Sucksdorff, M., Airas, L., 2022. Innate immune cell-related pathology in the thalamus signals a risk for disability progression in multiple sclerosis. Neurology(R) Neuroimmunol. Neuroinflammation 9, e1182. https://doi.org/10.1212/NXI.0000000000001182.
O'Loughlin, E., Madore, C., Lassmann, H., Butovsky, O., 2018. Microglial phenotypes and functions in multiple sclerosis. Cold Spring Harb. Perspect. Med. 8 https://doi.org/10.1101/CSHPERSPECT.A028993.
Politis, M., Giannetti, P., Su, P., Turkheimer, F., Keihaninejad, S., Wu, K., Waldman, A., Malik, O., Matthews, P.M., Reynolds, R., Nicholas, R., Piccini, P., 2012. Increased PK11195 PET binding in the cortex of patients with MS correlates with disability. Neurology 79, 523–530. https://doi.org/10.1212/WNL.0B013E3182635645.
Ransohoff, R.M., Schafer, D., Vincent, A., Blachère, N.E., Bar-Or, A., 2015. Neuroinflammation: ways in which the immune system affects the brain. Neurotherapeutics 12, 896–909. https://doi.org/10.1007/s13311-015-0385-3.
Rissanen, E., Tuisku, J., Rokka, J., Paavilainen, T., Parkkola, R., Rinne, J.O., Airas, L., 2014. *In vivo* detection of diffuse inflammation in secondary progressive multiple sclerosis using pet imaging and the [11C]PK11195. J. Nucl. Med. 55, 939–944. https://doi.org/10.2967/jnumed.113.131698.
Rissanen, E., Tuisku, J., Vahlberg, T., Sucksdorff, M., Paavilainen, T., Parkkola, R., Rokka, J., Gerhard, A., Hinz, R., Talbot, P.S., Rinne, J.O., Airas, L., 2018. Microglial activation, white matter tract damage, and disability in MS. Neurology - Neuroimmunol. Neuroinflammation 5. https://doi.org/10.1212/nxi.0000000000000443 e443.
Scalfari, A., Neuhaus, A., Daumer, M., Muraro, P.A., Ebers, G.C., 2014. Onset of secondary progressive phase and long-term evolution of multiple sclerosis. J. Neurol. Neurosurg. Psychiatry 85, 67–75. https://doi.org/10.1136/jnnp-2012-304333.
Schmidt, P., Gaser, C., Arsic, M., Buck, D., Förschler, A., Berthele, A., Hoshi, M., Ilg, R., Schmid, V.J., Zimmer, C., Hemmer, B., Mühlau, M., 2012. An automated tool for detection of FLAIR-hyperintense white-matter lesions in Multiple Sclerosis. Neuroimage 59, 3774–3783. https://doi.org/10.1016/j.neuroimage.2011.11.032.
Scolding, N., Barnes, D., Cader, S., Chataway, J., Chaudhuri, A., Coles, A., Giovannoni, G., Miller, D., Rashid, W., Schmierer, K., Shehu, A., Silber, E., Young, C., Zajicek, J., 2015. Association of british neurologists: revised (2015) guidelines for prescribing disease-modifying treatments in multiple sclerosis. Pract. Neurol. 15, 273–279. https://doi.org/10.1136/practneurol-2015-001139.
Sucksdorff, M., Matilainen, M., Tuisku, J., Polvinen, E., Vuorimaa, A., Rokka, J., Nylund, M., Rissanen, E., Airas, L., 2020. Brain TSPO-PET predicts later disease progression independent of relapses in multiple sclerosis. Brain 143, 3318–3330. https://doi.org/10.1093/brain/awaa275.
Sucksdorff, M., Tuisku, J., Matilainen, M., Vuorimaa, A., Smith, S., Keitilä, J., Rokka, J., Parkkola, R., Nylund, M., Rinne, J., Rissanen, E., Airas, L., 2019. Natalizumab treatment reduces microglial activation in the white matter of the MS brain. Neurology(R) Neuroimmunol. Neuroinflammation 6. https://doi.org/10.1212/NXI.0000000000000574.
Tremlett, H., Zhao, Y., Devonshire, V., 2008. Natural history of secondary-progressive multiple sclerosis. Multiple Sclerosis J. 14, 314–324. https://doi.org/10.1177/1352458507084264.
Turkheimer, F.E., Edison, P., Pavese, N., Roncaroli, F., Anderson, A.N., Hammers, A., Gerhard, A., Hinz, R., Tai, Y.F., Brooks, D.J., 2007. Reference and target region modeling of [11 C]-(R)-PK11195 brain studies. J. Nuclear Med. 48, 158–167.
Uher, T., Vaneckova, M., Sobisek, L., Tyblova, M., Seidl, Z., Krasensky, J., Ramasamy, D., Zivadinov, R., Havrdova, E., Kalincik, T., Horakova, D., 2017. Combining clinical and magnetic resonance imaging markers enhances prediction of 12-year disability in multiple sclerosis. Mult. Scler. 23, 51–61. https://doi.org/10.1177/1352458516642314.